Photoactivated 3-Azioctanol Irreversibly Desensitizes Muscle Nicotinic ACh Receptors *via* Interactions at αE262†

Stuart A. Forman,*,‡,§ Qiong L. Zhou,|| and Deirdre S. Stewart‡

Department of Anesthesia & Critical Care, Jackson 4, Massachusetts General Hospital, Boston, Massachusetts 02114, Department of Anaesthesia, Harvard Medical School, Boston, Massachusetts 02114, and Program in Molecular Medicine, University of Massachusetts Medical School, 373 Plantation Street, Worcester, Massachusetts 01605

Received June 29, 2007; Revised Manuscript Received August 14, 2007

ABSTRACT: 3-Azioctanol is a photoactivatable analogue of octanol that noncompetitively inhibits nicotinic acetylcholine receptors (nAChRs). Photolabeling studies using [^{3}H]-3-azioctanol in *Torpedo* nAChR identified αE262 as a site of desensitization-dependent incorporation. However, it is unknown whether photolabeling of αE262 causes functional effects in nAChRs and what other roles this residue plays in gating, desensitization, and channel block. We used ultrafast patch-perfusion electrophysiology and ultraviolet (UV) irradiation to investigate the state-dependence of both reversible nAChR inhibition by 3-azioctanol and the irreversible effects of photoactivated 3-azioctanol. Channels with mutations at αE262 were studied to determine ACh EC50s, desensitization rates, and sensitivities to reversible and photoirreversible 3-azioctanol inhibition. Exposure to 3-azioctanol in the presence of 365 nm UV light produced irreversible inhibition of wild-type nAChRs. Desensitization with ACh dramatically increased the degree of irreversible inhibition by photoactivated 3-azioctanol. Mutations at αE262 that reduce diazirine photomodification decreased the irreversible inhibition induced by photoactivated 3-azioctanol. Hydrophobic mutations at αE262 significantly slowed rapid ACh-induced desensitization and dramatically slowed fast resensitization. In contrast, αE262 mutations minimally affected 3-azioctanol channel block, and a half blocking concentration of 3-azioctanol did not alter the rate of ACh-induced fast desensitization. Our results indicate that position αE262 on muscle nAChRs contributes to an allosteric modulator site that is strongly coupled to desensitization. Occupation of this pocket by hydrophobic molecules stabilizes a desensitized state by slowing resensitization.

Muscle nicotinic acetylcholine receptors (nAChRs[1]) are among the best understood ligand-gated ion channel membrane proteins, providing structural and functional insight into the cys-loop superfamily including neuronal nAChRs, γ-amino butyric acid type A receptors ($GABA_AR$), serotonin type 3 receptors, (5HT3R), and glycine receptors (GlyR) (*1*). Structurally, peripheral nAChRs consist of 5 homologous subunits ($\alpha\gamma\alpha\delta\beta$ or $\alpha\gamma\alpha\epsilon\beta$), each containing a large N-terminal agonist-binding domain, four transmembrane domains (M1−M4), and a large intracellular domain between M3 and M4 (*2*). Detailed structural models for the resting (closed) receptor have emerged from electron photomicrographic analysis of nAChRs purified from *Torpedo* electroplaque (*3*) and high-resolution X-ray crystallographic studies of the ACh binding protein (AChBP) from snail (*4*). Agonist binding to muscle nAChRs triggers channel opening in under a millisecond, followed by desensitization that occurs in several phases over seconds to minutes. Desensitized states are nonconducting, but characterized by high affinity for agonists and a number of other ligands, including various noncompetitive inhibitors. Nicotinic AChR desensitization and allosteric sites that affect this process are growing areas of interest because channel desensitization is thought to play a role in myopathies, epilepsy, drug addiction, and other central nervous system diseases (*5*−*9*).

Noncompetitive nAChR inhibitors, which include a wide range of neuromodulatory compounds, can impair receptor function by blocking ion conductance through open channels and/or by allosterically stabilizing the inactive resting and desensitized states. This study focuses on 3-azioctanol, a photolabel analogue of *n*-octanol with similar nAChR inhibitory potency (*10*) and very likely the same mechanism(s) of inhibition. The major site of 3-azioctanol photoincorporation into *Torpedo* nAChRs is known (*11*), but the functional consequences of this covalent modification are not known.

Octanol and other long-chain alcohols noncompetitively and reversibly inhibit nAChRs *via* both channel block and desensitization. Channel block by *n*-octanol is characterized by an IC50 near 25 μM. State-dependence studies show that *n*-octanol block occurs *after* channel activation (*12*), and

† This research was supported by the MGH Dept. of Anesthesia & Critical Care and grants from NIH to S.A.F. (GM66724 and GM58448).

* Correspondence should be addressed to this author: Dept. of Anesthesia & Critical Care, Jackson 4, Mass. General Hospital, Boston, MA 02114; e-mail, saforman@partners.org; phone, 617-724−5156; fax, 617-724−8644.

‡ Massachusetts General Hospital.

§ Harvard Medical School.

|| University of Massachusetts Medical School.

[1] Abbreviations: 3-AO, 3-azioctanol [3-(2-hydroxyethyl)-3-*n*-pentyldiazirine]; ACh, acetylcholine; EC50, 50% effect concentration; IC50, 50% inhibitory concentration; nAChR, nicotinic acetylcholine receptor; UV, ultraviolet.

10.1021/bi701287a CCC: $37.00
Published on Web 10/02/2007

single-channel studies confirm that the duration of blocked periods within channel openings correlates with anesthetic and alcohol potency (*13*). A region near the middle of the α subunit M2 domain (L251 to V255) that largely determines receptor sensitivity to alcohol block (*14*) was mapped by hydrophobic mutagenesis. Similar mutation studies on the other nAChR subunits indicate that the conductive channel itself is the site of block by long-chain alcohols (*15*).

In comparison to channel block, far less is known about the mechanism of nAChR desensitization by *n*-octanol. In the absence of agonists, *n*-octanol directly induces desensitization of *Torpedo* nAChRs with an EC50 of 490 μM, a concentration sufficient to perturb lipid membranes (*16*). Alternatively, desensitization may be mediated by *n*-octanol binding to allosteric sites. *Torpedo* nAChR photolabeling with [^{3}H]-3-azioctanol has identified a potentially important candidate site (*11*). The majority of [^{3}H]-3-azioctanol radioactivity incorporated at a single residue on α subunits, αE262. Photoincorporation at αE262 was strongly enhanced under desensitizing conditions, induced with either orthosteric nAChR agonists or high concentrations of 3-azioctanol. Thus, rearrangements involving αE262 or nearby structures apparently occur during *Torpedo* nAChR desensitization, and homologous sites may exist in mammalian muscle and neuronal receptors. αE262 is located at the extracellular end of the pore-forming M2 domain, 7 to 11 amino acids from the region thought to form the open-channel block site. Mutations at αE262 have been reported to alter single-channel conductance and Mg^{2+} block (*17*), suggesting that it may contribute to long-chain alcohol block. Nearby residues in the M2−M3 linker are also thought to transduce agonist binding into transmembrane domain movements that initiate conductance gating of ligand-gated ion channels (*18*, *19*).

Our experiments aimed at defining the mechanism of reversible 3-azioctanol block and the functional impact of nAChR photomodification with 3-azioctanol. We also investigated the role of αE262 in nAChR gating and desensitization, as well as 3-azioctanol channel block. We studied recombinantly expressed wild-type and mutant muscle nAChRs using voltage-clamp electrophysiology in excised outside-out membrane patches. We used ultrafast (submillisecond) superfusate exchange to measure ACh-activated multichannel current amplitude and rates of desensitization and resensitization, state-dependent reversible 3-azioctanol inhibition, and 3-azioctanol effects on fast ACh-induced desensitization. We investigated the functional effects of exposing wild-type and mutant nAChRs to photoactivated 3-azioctanol, by irradiation with 365 nm light.

EXPERIMENTAL PROCEDURES

Animal Use. Female *Xenopus laevis* were housed in a veterinary-supervised environment in accordance with local and federal guidelines and with the approval of the institutional research animal care committee. Oocytes were harvested via minilaparotomy from frogs anesthetized with cold 0.2% tricaine.

Chemicals. 3-Azioctanol was a gift from Shaukut Husain, PhD (Massachusetts General Hospital, Boston, MA). Stock solutions in ethanol were kept in dark glass vials at −30 °C and used to prepare aqueous solutions in extracellular buffer within 2 h before use. The highest concentration of ethanol after dilution was 0.5% v/v, which had no effect on nAChR desensitization. Ethanol is known to enhance gating of nAChRs at low ACh concentrations, but does not alter responses to the saturating ACh concentrations used when 3-azioctanol was studied. All other chemicals were purchased from Sigma-Aldrich (St. Louis, MO)

Site-Directed Mutagenesis. cDNAs for α, β, γ, and δ subunits of the mouse muscle nAChR were subcloned into pSP64T plasmids. Mutant cDNAs were constructed using oligonucleotide-directed mutagenesis and confirmed by dideoxynucleotide sequencing.

Xenopus Oocyte Expression. Methods for oocyte expression were previously described (*12*). After incubation for 48−72 h, oocytes were stripped of their vitelline membranes prior to patch−clamp electrophysiology.

Patch−Clamp Electrophysiology. Multichannel currents were recorded from excised outside-out oocyte membrane patches at room temperature (20−22 °C). Patch pipettes were fire-polished to give open tip resistance of 2−5 MΩ. Oocyte patches were voltage-clamped at −50 mV, and rapid superfusate switching (0.4 to 0.8 ms, measured with open pipet junction currents) was achieved using a piezo-driven quad tube as described previously (*20*). Pipet and outside solutions were symmetrical K-100 (in mM: 97 KCl, 1 $MgCl_2$, 0.2 EGTA, 5 K-HEPES, pH adjusted to 7.5 with KOH). Currents through the patch−clamp amplifier (Axopatch 200A or 200B; Molecular Devices, Sunnyvale, CA) were filtered (8-pole bessel, 2−5 kHz) and digitized at 5−10 kHz. Current recordings were averaged from 3 to 12 (depending on current amplitude) sweeps, with 20−40 s between sweeps for recovery from desensitization.

ACh concentration responses were assessed using a 3-solution protocol that enabled intrasweep normalization (*21*). Channels were first activated with a low concentration of ACh, and immediately after peak current was reached, the patch was superfused with a high ACh concentration (1 mM) to elicit a maximal response. Activation rates at EC50 were all more than twenty times the fast desensitization rates, indicating that the EC50 is accurately determined with this technique. For each channel studied, leak-corrected and normalized data from at least 4 patches were combined and fit with a logistic equation to determine EC50 and Hill coefficient (eq 1).

$$\frac{I}{I_{max}} = \frac{1}{1 + \left(\frac{EC50}{[ACh]}\right)^n} \quad (1)$$

Rapid reversible 3-azioctanol inhibition was studied using a 3-solution "notch protocol." Channels were activated with a maximal ACh concentration (1 mM), and superfusate was then switched to one containing 1 mM ACh plus 30 μM 3-azioctanol (approximately IC50 in wild-type), and then back to ACh alone. The fraction of block was estimated from the ratio of currents immediately before adding 3-azioctanol and after inhibition reached steady-state (5−10 ms later). In the experiments assessing rapid block in single versus double-mutant channels, notch experiments were performed with different 3-azioctanol concentrations to construct a concentration−response curve. Normalized data from multiple

patches were combined and analyzed by nonlinear least-squares fitting to an inhibitory logistic function (eq 2).

$$\frac{I}{I_{max}} = \frac{1}{1 + \left(\frac{[3 - AO]}{IC50}\right)^n} \quad (2)$$

Photomodification with 3-Azioctanol. Irreversible modification by photoactivated 3-azioctanol was performed on individual excised patches during voltage-clamp electrophysiology experiments. Maximal currents were first elicited with 50−100 ms pulses of 1 mM ACh at 2 min intervals until minimal rundown (<1% per minute) was observed. Patches were then exposed to (a) UV light and K-100 buffer for 5 min, (b) 3-azioctanol for 5 min followed by 5 min wash in K-100 buffer, or (c) 3-azioctanol plus UV light for 5 min followed by 5 min wash. Three brief maximal ACh-elicited currents (at 30 s intervals) were recorded after each treatment to establish the fraction of the original current remaining. Irradiation of patches was achieved using a long-wavelength (365 nm peak) UV lamp (0.16 ampere handheld; model UVL-56, UVP, Upland, CA) that was positioned 5 cm above the flow chamber on the patch−clamp setup. 3-Azioctanol was superfused onto the patch via one of the four capillaries of the quad superfusion device. To study the impact of desensitization on irreversible 3-azioctanol photoinhibition, we established baseline maximal current and then exposed patches first to 1 mM ACh for 10 s followed by 1 mM ACh plus azioctanol for 5 min during UV irradiation. Current response was reassessed following 5−10 min wash.

Fast desensitization rates were estimated from traces recorded during long (5−20 s) pulses of saturating (1 mM) ACh. Recovery from fast desensitization (induced with a 5 s ACh pulse) was studied with standard double pulse protocols, where the amplitude of the second ACh pulse following a variable recovery period was normalized to that of the desensitizing pulse in each sweep. Sweeps (total of 10 s) were initiated at 30 s intervals. Recovery from slow desensitization (5 min) was studied by manually switching to 1 mM ACh superfusate during the 5 min desensitizing exposure and then immediately initiating a recording protocol of 12 short (100 ms) ACh activation sweeps at fixed intervals.

Data Analysis and Statistics. Sweeps were examined and analyzed off-line. Desensitization and resensitization (recovery) time constants were determined from nonlinear least-squares fits with one, two, or three exponential component equations:

$$I = A_1 e^{-t/\tau 1} + A_2 e^{-t/\tau 2} + A_3 e^{-t/\tau 3} + I_\infty \quad (3)$$

The number of fitted exponential components was determined by comparing models using F-tests at $P > 0.98$ (Clampfit 9.0; Molecular Devices, Sunnyvale, CA, or GraphPad Prism; GraphPad Software, San Diego, CA). To compare desensitization or resensitization when there were different numbers of exponential components, a weighted average time constant was calculated:

$$\tau_w = \frac{\sum_{i=1}^{n} A_i \tau_i}{\sum_{i=1}^{n} A_i} \quad (4)$$

All results are reported as mean ± standard deviation, unless otherwise indicated. Results for 3-azioctanol reversible inhibition, irreversible photoinhibition, and fast desensitization τ_w data for wild-type and mutant nAChRs were compared using ANOVA with Tukey's post-hoc multiple comparisons test in MS Excel (Microsoft Corp., Remond, WA) with an add-on statistical toolkit (StatistiXL; www.statistixl.com). ACh EC50s for mutants versus wild-type were compared pairwise in logistic fits (eq 1) using GraphPad Prism software (GraphPad Software, San Diego, CA).

RESULTS

Reversible Inhibition of Wild-Type Receptors. Outside-out voltage-clamped membrane patches were excised from *Xenopus* oocytes expressing wild-type mouse $\alpha\gamma\alpha\delta\beta$ nAChRs and multichannel currents were stimulated with submillisecond superfusate switching using a custom-built quad 2 × 2 capillary array. Brief pulses of saturating ACh (1 mM) elicited rapid inward currents (Figure 1, top) that desensitized with time constants ranging from 80 to 180 ms (av ± SD = 140 ± 55 ms; $n = 9$). Reversible channel inhibition was studied using a "notch" protocol as described in Experimental Procedures (Figure 1, middle). Inhibition by 30 μM 3-azioctanol was complete within 5 ms, and recovery from inhibition was complete within 8−10 ms. Recovery currents following "notch" applications of 3-azioctanol closely matched those elicited with ACh alone (Figure 1, middle), demonstrating that the rate of ACh-induced rapid desensitization was unaltered by 3-azioctanol blockade. Some patches were also subjected to a "pre-exposure" protocol where exposure to 3-azioctanol preceded activation by ACh (Figure 1, bottom). Currents elicited following 3-azioctanol pre-exposure displayed biphasic current decay immediately after ACh application. The fast phase represents development of 3-azioctanol inhibition, showing that 3-azioctanol inhibition mostly occurs after channel activation, as previously shown for *n*-octanol (*12*). The slow phase parallels desensitization in notch experiments and is characterized by similar time constants (100 to 180 ms) during longer pulses with ACh plus 3-azioctanol.

Wild-Type Receptor Recovery from Desensitization Induced by ACh vs 3-Azioctanol Exposure. Full agonists, such as ACh, induce desensitization of wild-type nAChRs in several phases: a fast phase with a time constant of about 140 ms, and a slow phase with a time constant of seconds. Recovery from agonist-induced desensitization is also multiphasic (Figure 2, top). Following desensitization by 1 mM ACh exposure for 5 s, we found that recovery is mostly complete within 5−6 s (τfast = 0.8 ± 0.38 s; Afast = 0.85 ± 0.08; $n = 5$) with a second slow recovery component characterized by τslow = 6 ± 1.2 s and Aslow = 0.15 ± 0.07 ($n = 5$). Recovery following 5 min of ACh exposure was slower due to a dominant slow component (Aslow = 0.80 ± 0.12; $n = 5$) with a time constant of 9 ± 2.3 s (n =

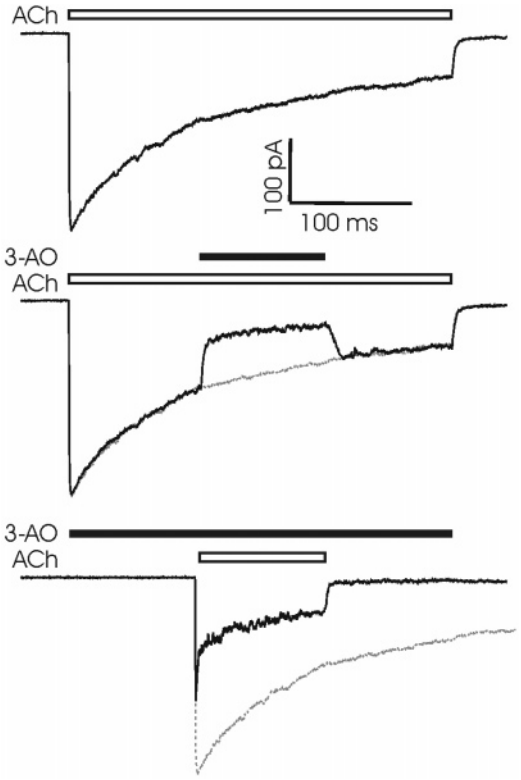

FIGURE 1: Reversible nAChR channel inhibition by 3-azioctanol. Three current traces are shown, recorded from the same patch expressing wild-type muscle nAChRs. Open bars above traces indicate application of 1 mM ACh, and solid bars indicate 30 μM 3-azioctanol. Top: A current trace elicited with a 250 ms pulse of ACh, showing rapid activation of inward current, desensitization (τ = 140 ms), and rapid deactivation following cessation of ACh. Middle: A "notch" protocol showing rapid onset and recovery from inhibition by 3-azioctanol. Note that following recovery from inhibition, the trace is indistinguishable from the control (dotted trace), indicating no change in desensitization rate. Bottom: After pre-exposure to 3-azioctanol, ACh-activated currents show two phases of inhibition. The fast phase is the onset of open-channel block, and the slower phase parallels desensitization in the absence of inhibitor (dotted trace).

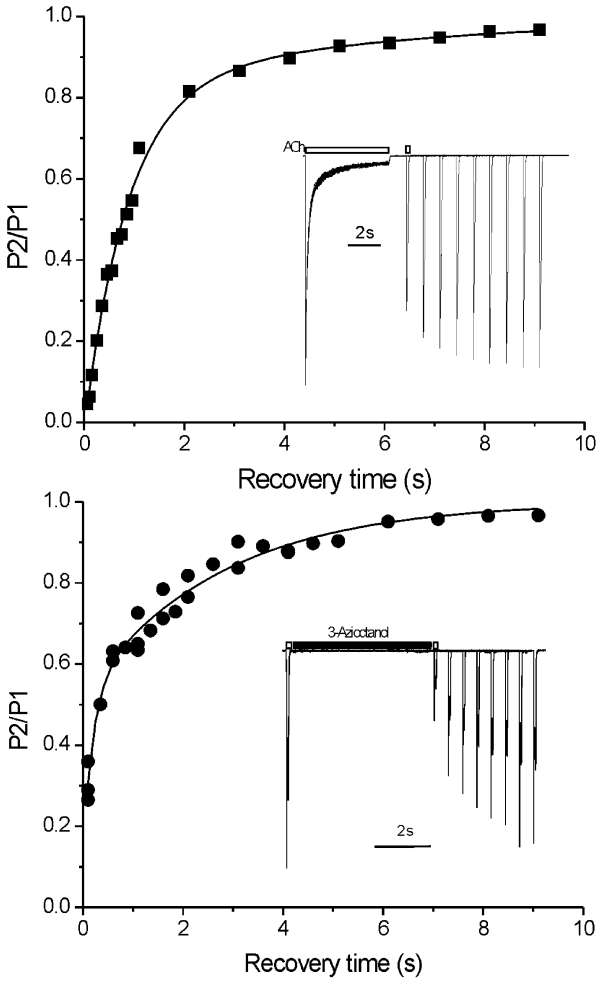

FIGURE 2: Reversible wild-type nAChR Desensitization by ACh and 3-azioctanol. Top: Data is from a single patch studied using a "double pulse" protocol with a 5 s desensitizing pulse (P1 = peak) of 1 mM ACh followed by variable wash periods and then a 50 ms pulse (P2 = peak) to test recovery. The plotted recovery ratios P2/P1 were combined from two experiments on the same patch using recovery time increments of either 100 ms or 1 s. Multiphasic desensitization is evident in the traces shown in the inset, along with recovery pulses spaced 1 s apart. The weighted average time constant (τ_w) for desensitization of this patch (20 sweeps) was 150 ms. ACh application is depicted by the open bars above the traces. Resensitization shows 2 phases characterized by τfast = 0.87 s, Afast = 0.84, τslow = 5.8 s, Aslow = 0.17. Bottom: Data is from another patch subjected to the following 5-part protocol: (1) 50 ms prepulse of 1 mM ACh; (2) 100 ms buffer wash; (3) 5 s exposure to 600 μM 3-azioctanol; (4) variable buffer wash period; (5) 50 ms recovery test pulse. Application of ACh and 3-azioctanol are depicted respectively by open and solid bars above the traces in the inset. The plotted recovery ratios P2/P1 were combined from three experiments on the same patch using recovery time increments of 250 ms, 500 ms, and 1 s. Recovery from desensitization induced by 3-azioctanol shows two phases characterized by by τfast = 0.20 s, Afast = 0.40, τslow = 2.7 s, Aslow = 0.47.

5). High concentrations of 3-azioctanol also desensitize muscle nAChRs. Following a 5 s exposure to 600 μM 3-azioctanol, ACh response was 25−35% of maximum after 50 ms of wash and recovery proceeded in two phases (Figure 2, bottom) with time constants of 0.3 ± 0.14 s (Afast = 0.43 ± 0.064; n = 5) and 3 ± 1.3 s (Aslow = 0.51 ± 0.10; n = 5). Recovery of full ACh response following 5 min exposure to 3-azioctanol (100−600 μM) was complete in about 15−30 s with a dominant component characterized by τ = 6 ± 2.0 s (n = 5).

Irreversible Inhibition of Wild-Type Receptors by Photoactivated 3-Azioctanol. Five minute exposure to desensitizing concentrations (600 μM) of photoactivated (365 nm light) 3-azioctanol irreversibly inhibited wild-type nAChRs (Figure 3 top). No irreversible inhibition was evident following 5 min exposure to 365 nm light alone or to 5 min exposure to 3-azioctanol alone followed by a 5 min wash. When both 3-azioctanol and UV light were present together, subsequent patch currents were reduced on average 39 ± 6.1% (n = 6) from pretreatment controls. Further washing (up to 20 min) did not result in more recovery of peak currents (not shown). Repeated exposures to photoactivated 3-azioctanol produced more nAChR inhibition, with near complete loss of ACh response following cumulative exposures of 30 min under these conditions (not shown).

Irreversible inhibition of nAChRs was sensitive to both the concentration of 3-azioctanol and to the presence of ACh (Figure 3 middle and bottom). Five minute exposure to 200 μM photoactivated 3-azioctanol resulted in a modest amount of irreversible inhibition of wild-type currents (11 ± 5%; n = 4), which was significantly less than that produced using 600 μM (p < 0.001). When 200 μM photoactivated 3-azioctanol was coapplied with 1 mM ACh for 5 min followed

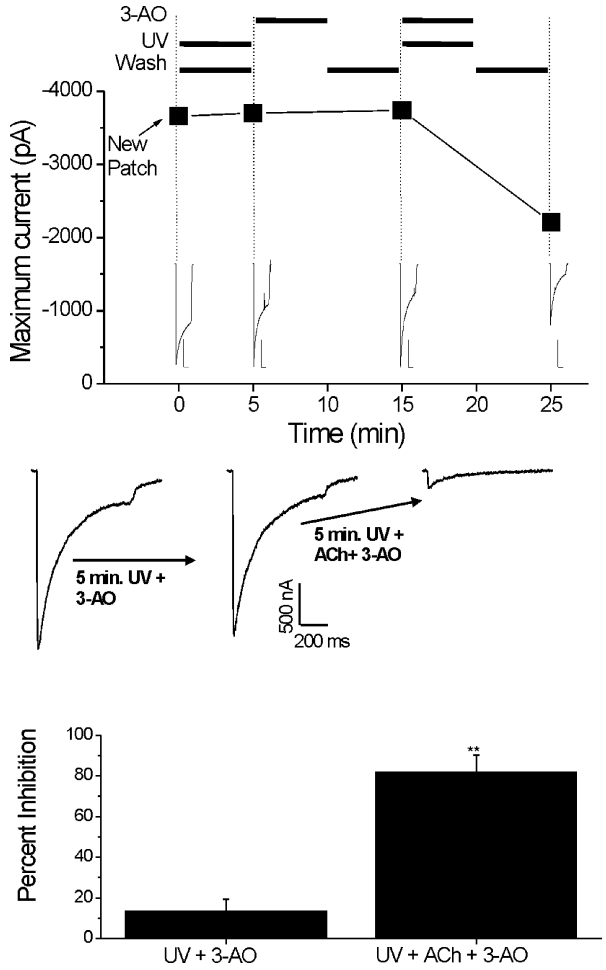

FIGURE 3: Irreversible nAChR inhibition by photoactivated 3-azioctanol. Top: Peak response data from a single patch expressing wild-type muscle nAChRs is shown. Responses were first shown to be stable for 5 min (0 time point), and peak currents were retested at intervals following 5 min exposure to 365 nm light (5 min time point), 5 min exposure to 600 μM 3-azioctanol followed by 5 min buffer wash (15 min time point), and 5 min exposure to both 365 nm light plus 3-azioctanol followed by 5 min wash (25 min time point). A reduction in peak current was only observed following exposure to photoactivated 3-azioctanol. Middle: Three traces from another patch are shown illustrating the impact of 5 min exposure to photoactivated 3-azioctanol (200 μM) in the absence versus presence of ACh. The pretest response is shown on the left and 8% inhibition is observed following photoactivated 3-azioctanol. Additional exposure to photoactivated 3-azioctanol plus 1 mM ACh resulted in a 91% drop in current response. Bottom: Summary of irreversible inhibition by 200 μM photoactivated 3-azioctanol in the absence versus presence of 1 mM ACh.

by 5−10 min wash, 84 ± 7% (n = 4) of current was irreversibly lost, an 8-fold increase in inhibition relative to that in the absence of ACh. In control experiments where 3-azioctanol and ACh were coapplied without UV light, currents recovered fully following wash.

αE262 Mutant Effects on ACh EC50 and Fast Desensitization. Seven mutations were introduced at α262, and the impact of these mutations on ACh sensitivity (agonist EC50), fast ACh-induced desensitization, and reversible inhibition by 30 μM 3-azioctanol was investigated. Results are summarized in Table 1. Three mutations reduced ACh EC50: αE262Q, αE262T, and αE262D. One mutation, αE262L, modestly increased EC50. Five mutations, αE262V, αE262L, αE262W, αE262T, and αE262Q, significantly prolonged desensitization. We also studied recovery from fast desensitization in αE262L. In comparison to wild-type receptors, αE262L mutant channels recovered much more slowly from desensitization (Figure 4). The αE262L recovery time constant following ACh-induced desensitization was 6 ± 1.3 s (n = 3), and a fast recovery component was absent.

αE262 Mutant Effects on Reversible Inhibition by 3-Azioctanol. For all but one of the αE262 mutant channels the degree of fast reversible inhibition by 30 μM 3-azioctanol was not significantly different from wild-type. The αE262T mutation modestly, but significantly (p = 0.03), reduced reversible inhibition by 3-azioctanol (Figure 5; Table 1). The reduced inhibition in receptors containing the αE262T mutation suggests about a 2-fold increase in IC50 relative to wild-type (50 μM for αE262T vs 25μM for wild-type).

Previous studies have shown that M2 mutations at αS252 and αL251 dramatically affect nAChR sensitivity to reversible inhibition by long-chain alcohols (*14*). This is also the case for inhibition by 3-azioctanol (Figure 5 top). Receptors containing the αS252I mutation were much more sensitive than wild-type to 30 μM 3-azioctanol, displaying 90 ± 5.7% (n = 4; p < 0.001) reversible inhibition. In addition, receptors containing the αL251V mutation were reversibly inhibited only 29 ± 5.2% (n = 4; p < 0.001) by 30 μM 3-azioctanol.

To test whether 3-azioctanol inhibition was additively affected by αE262 and αS252 mutations, we created a double αS252I + E262T mutant and compared its sensitivity to 3-azioctanol with that of the αS252I single mutant (Figure 5, bottom). In notch experiments, the αS252I + E262T mutant was inhibited 93 ± 6.3% (n = 6) at 30 μM 3-azioctanol and 3-azioctanol IC50s estimated from concentration−response studies in αS252I + E262T and αS252I were not significantly different (1.4 ± 0.3 μM vs 2.1 ± 0.4 μM; p = 0.23).

αE262 Mutant Effects on Irreversible Inhibition by Photoactivated 3-Azioctanol. Irreversible UV-dependent inhibition by 600 μM 3-azioctanol was investigated in four αE262 mutants. Because diaziryl photolabels preferentially react with nucleophilic atoms in their environment, we studied one mutant that maintained side chain electronegativity, αE262D, and three that reduced this property, αE262V, αE262Q, and αE262L. We found that UV-dependent irreversible inhibition of αE262D by 3-azioctanol was the same as that in wild-type, while significantly less irreversible inhibition was observed in the mutants that reduced side-chain electronegativity at α262 (Table 1).

DISCUSSION

We investigated the functional role of αE262, an outer M2-domain residue of nAChR, in two different modes of inhibition by 3-azioctanol, a photoactivatable noncompetitive inhibitor, as well as in ACh-induced gating and desensitization. Our results reveal that 3-azioctanol inhibits nAChRs *via* two mechanisms associated with distinct sites. The αE262 residue contributes to a site that is coupled to nAChR desensitization/resensitization, but is not involved in rapid reversible channel block, which is mediated by a previously described site (*14*).

To investigate the effects of 3-azioctanol at αE262, we utilized mutagenesis and photomodification in combination with ultrafast patch perfusion electrophysiology. Photoactivatable ligands provide tools for real-time functional modi-

Table 1: Summary of Results for αE262 Mutations[a]

α262 side chain	ACh EC50 (μM)	desensitization τ_w (ms)	3-AO inhibition (%)	
			reversible	irreversible
glutamate (E); (wild-type)	18 ± 2.1	140 ± 45 (5)	55 ± 7.1 (9)	39 ± 6.1 (6)
aspartate (D)	9 ± 3.5*	90 ± 25 (4)	41 ± 7.4 (4)	41 ± 12 (4)
threonine (T)	3.1 ± 0.4**	440 ± 110** (4)	38 ± 4.4* (4)	nd[b]
valine (V)	14 ± 5.2	390 ± 97** (5)	53 ± 11 (5)	20 ± 3.5** (5)
leucine (L)	29 ± 3.5*	280 ± 44* (4)	52 ± 10 (5)	19 ± 5.7** (5)
tryptophan (W)	23 ± 4.8	240 ± 35* (4)	53 ± 4.7 (4)	nd
glutamine (Q)	4 ± 1.2**	380 ± 85** (5)	45 ± 7.6 (5)	25 ± 4.8* (5)
lysine (K)	27 ± 7.8	90 ± 21 (4)	55 ± 11 (4)	nd

[a] Data are reported as mean ± SD (number of patches). *$p < 0.05$. **$p < 0.005$. Desensitization weighted time constants (τ_w) were calculated with eq 4 (Experimental Procedures). Reversible inhibition was measured using 30 μM 3-azioctanol (3-AO) and irreversible inhibition using 600 μM 3-azioctanol plus UV light. [b] Not determined.

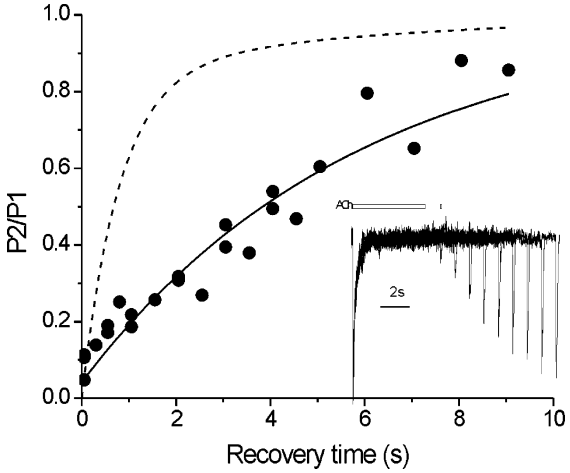

FIGURE 4: Desensitization recovery in αE262L mutant nAChRs. ACh-induced desensitization and recovery were studied using a "double pulse" protocol as described in Figure 2. ACh application is shown as open bars above traces in the inset. Desensitization during the 5 s ACh pulse is characterized by a weighted average τdes = 230 ms (24 sweeps). Recovery ratio (P2/P1) data are shown from 3 experiments on the same patch using 250 ms, 500 ms, and 1 s increments in recovery intervals. Recovery is monoexponential with a fitted time constant of 5.9 s (solid line). For comparison, wild-type recovery, based on average values, is shown as a dashed line.

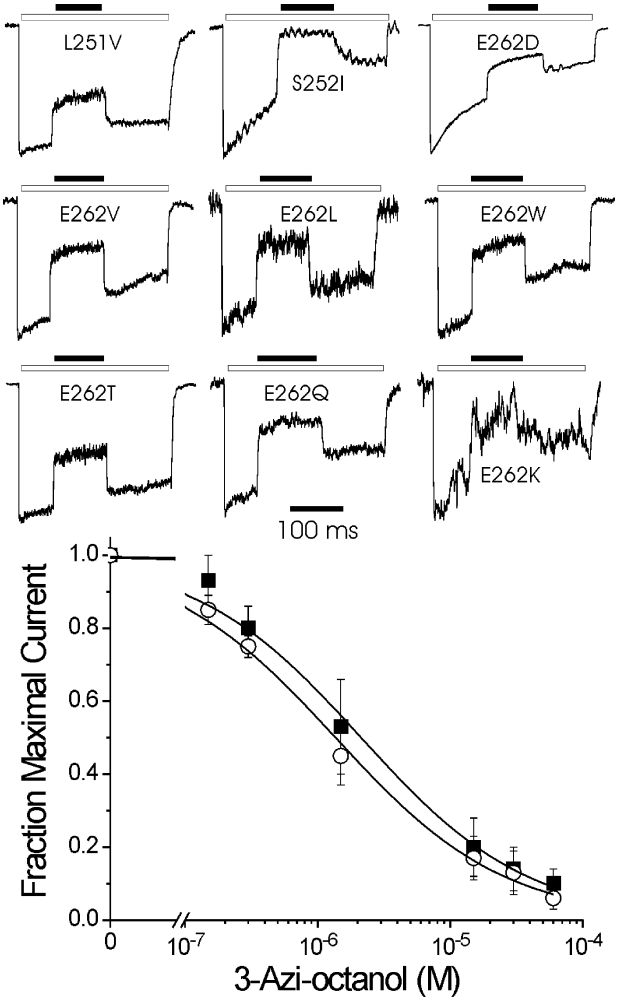

FIGURE 5: Effect on reversible nAChR inhibition of mutations at αE262 versus αL251 and αS252. Top: Panels depict sweeps from "notch" inhibition experiments using 30 μM 3-azioctanol for seven αE262 mutants as well as αL251V and αS252I. Two mutants, αL251V and αE262T, show significantly less inhibition than wild-type nAChR, and one mutant, αS2652I, shows significantly more inhibition than wild-type. Results are summarized in Table 1. Bottom: 3-Azioctanol inhibitory concentration−response data (mean ± SD; $n \geq 3$) is shown for the αS2652I mutant (open circles) and the αS2652I+αE262T double mutant (solid squares). Lines through the data represent logistic fits. The fitted IC50s are not significantly different (see text).

fication with further potential for providing spatial control of modification within cellular networks. The specificity of the photoactivatable ligand for its target is important, and in this study, we addressed specificity by incorporating mutations at the presumed molecular site of incorporation (see below). The combination of photomodification with patch−clamp electrophysiology has previously been reported using agonists at both CNG channels (*22*, *23*) and nAChRs (*24*, *25*). We are unaware of other studies where photoactivated ion channel inhibitors have been studied using a combination of electrophysiology and incorporation-site mutations.

Our results demonstrate that the irreversible inactive state produced by 3-azioctanol photomodification at αE262 is a desensitized state. We found that exposure of nAChRs to 3-azioctanol in the presence of 365 nm light causes irreversible loss of function (Figure 3). This irreversible inhibition is dependent on 3-azioctanol concentration in the concentration range associated with *n*-octanol desensitization (*16*) and is also enhanced about 8-fold when ACh was used to promote desensitization, paralleling results from [^{3}H]-3-azioctanol photoincorporation at αE262 in *Torpedo* nAChR (*11*). The effects of mutations at αE262 are also consistent with a role in desensitization/resensitization as well as 3-azioctanol modification. Mutations at αE262 alter both desensitization/resensitization rates and the degree of irreversible inhibition caused by photoactivated 3-azioctanol (Table 1). We studied

an insufficient number of mutations to reach conclusions regarding side-chain properties associated with changes in fast receptor desensitization, but it is notable that replacing glutamic acid with the hydrophobic side chains valine, leucine, and tryptophan caused slowing of fast desensitization. Hydrophobic mutations at αE262 also dramatically slowed recovery from fast desensitization, apparently by reducing or eliminating the fastest recovery component (Figure 4). This observation provides a direct correlate with the irreversible desensitization associated with 3-azioctanol modification, and strongly suggests that long-chain alcohols also slow recovery from desensitization.

Our strategy of hydrophobic mutagenesis to reduce or eliminate diazirine photomodification at αE262 was based on evidence that photoactivated alkyl diaziryls are electrophilic, explaining the large numbers of tyrosines, glutamates, and aspartates, but little or no aliphatic side chains identified using such photolabels (*26*). Reducing electronegativity at α262, by mutation to valine, leucine, and glutamine, was associated with significantly reduced irreversible inhibition by photoactivated 3-azioctanol (Table 1). Based on our observation that the αE262L mutation slows resensitization far more than desensitization, we infer that αE262L desensitizes more completely than wild-type in the presence of agonists. Furthermore, the reduced irreversible desensitization by photoactivated 3-azioctanol seen in αE262L and other mutant channels cannot be attributed to a reduced tendency to desensitize, because wild-type and mutant nAChRs we studied all reversibly desensitize more than 95%. Thus, reduced irreversible desensitization in αE262 mutants likely reflects a reduced ability to form covalent bonds with photoactivated 3-azioctanol, and may also reflect altered binding of azioctanol at this site. In addition, the αE262 mutations that we studied did not fully eliminate irreversible inactivation by 3-azioctanol. This result could reflect a simple reduction in the degree of modification, perhaps by reacting with other less electronegative amino acids at the mutated site. Alternatively, other sites of 3-azioctanol modification (*11*) may irreversibly influence receptor function.

The results discussed above demonstrate that both *Torpedo* electroplaque and mammalian muscle nAChRs have homologous alcohol binding sites that include αE262 and that are coupled to desensitization. Other noncompetitive nAChR inhibitors are known to induce or affect the degree of nAChR desensitization. In the case of quinacrine the major effect is to accelerate the forward rate of desensitization (*27*). Other desensitizing inhibitors, including crystal violet, have been proposed to interact at αE262 (*28*). Indeed, the α subunits of neuronal nAChRs all include a glutamic acid at the 20′ position of the M2 domain, suggesting the possibility that homologous desensitization-linked sites exist on neuronal receptor subtypes.

Other experiments described here examine rapidly reversible inhibition of nAChRs by low concentrations of 3-azioctanol, and the role of αE262 in this action. Previous studies (*12*, *14*, *15*) indicate that reversible inhibition by long-chain alcohols represents channel-block, and mutations near the middle of the α-M2 domain (from αL251 to αV255) strongly affect channel sensitivity. In the current study we observed that 30 μM 3-azioctanol reversibly and selectively blocks open nAChRs (Figure 1) and that mutations at αL251 and αS252 significantly alter channel sensitivity to block (Figure 5). Thus, our data show that 3-azioctanol and *n*-octanol display the same mechanism of channel block. Only one αE262 mutant (αE262T) demonstrated modestly altered sensitivity to reversible inhibition by 3-azioctanol, and this effect was not additive with that of another mutation near the middle of the α-M2 domain. We conclude that αE262 does not contribute to the midchannel alcohol blocking site or form a second block site.

Our observation that some mutations at αE262 alter fast ACh-induced desensitization without significantly changing ACh EC50 (Table 1) provides further evidence that agonist-induced gating and desensitization are associated with distinct structures that can be uncoupled. Previous studies have provided evidence that ion channel gating (open−close transitions) and desensitization are associated with independent structural rearrangements, while desensitization of wild-type nAChRs appears to be coupled to the open state (*29*). We and others have previously described α-M2 channel mutants that change ACh EC50 by altering the gating equilibrium (*14*, *30*). Some of these mutants (e.g., αL251T) also profoundly affect fast ACh-induced desensitization rates, indicating that portions of the α-M2 domain couple to both gating and desensitization. Similar observations have been made in $GABA_A$ receptors (*21*, *31*, *32*), suggesting that all ligand-gated ion channels in the cys-loop superfamily have independent gates for ion conductance and desensitization. Our data further demonstrate that block by 3-azioctanol does not affect the fast ACh-induced desensitization rate, indicating that blocked channels can desensitize at the same rate as open channels. Previously, Purohit and Grosman (*33*) reported that nAChR desensitization is unaffected by choline channel blockade, leading to a similar conclusion.

Photomodification of αE262 with 3-azioctanol stabilizes the desensitized state on the time scale of tens of minutes or longer, whereas the α262L mutation slows recovery on the time scale of seconds. This comparison suggests that the size of the αE262 side chain may be a determinant in stabilizing the desensitized state. Bond formation between 3-azioctanol and the carboxylate moiety of glutamate lengthens the original 3 carbon side chain, adding 6 carbons. This photomodified side chain is much longer than that of valine (2 carbons), leucine (3 carbons), or tryptophan (5−6 carbon effective length). The photomodified α262 side chain may be long enough to reach the alcohol blocking site, about 3 helical turns distant. However, because photoinhibition by 3-azioctanol is desensitization-dependent, but desensitization and channel block are independent, we find it unlikely that the resulting inactive receptors are irreversibly blocked. Studies using aliphatic diazirines of varying length may be useful in further testing this possibility.

ACKNOWLEDGMENT

We thank Dr. Shakut Husain (Massachusetts General Hospital) for providing 3-azioctanol. Professors Jonathan Cohen and Keith Miller (Harvard Medical School) provided useful discussions about photochemical selectivity and mechanisms. Technical assistance was provided by Carol Gelb and Aiping Liu.

REFERENCES

1. Sine, S. M., and Engel, A. G. (2006) Recent advances in Cys-loop receptor structure and function, *Nature 440*, 448−455.

2. Karlin, A. (2002) Emerging structure of the nicotinic acetylcholine receptors, *Nat. Rev. Neurosci. 3*, 102−114.
3. Unwin, N. (2005) Refined structure of the nicotinic acetylcholine receptor at 4Å resolution, *J . Mol. Biol. 346*, 967−989.
4. Brejc, K., van Dijk, W. J., Klaassen, R. V., Schuurmans, M., van Der Oost, J., Smit, A. B., and Sixma, T. K. (2001) Crystal structure of an ACh-binding protein reveals the ligand-binding domain of nicotinic receptors, *Nature 411*, 269−276.
5. Elenes, S., Ni, Y., Cymes, G. D., and Grosman, C. (2006) Desensitization contributes to the synaptic response of gain-of-function mutants of the muscle nicotinic receptor, *J. Gen. Physiol. 128*, 615−627.
6. Giniatullin, R., Nistri, A., and Yakel, J. L. (2005) Desensitization of nicotinic ACh receptors: shaping cholinergic signaling, *Trends Neurosci. 28*, 371−378.
7. Hogg, R. C., and Bertrand, D. (2004) Nicotinic acetylcholine receptors as drug targets, *Curr. Drug Targets: CNS Neurol. Disord. 3*, 123−130.
8. Martin, L. F., and Freedman, R. (2007) Schizophrenia and the alpha7 Nicotinic Acetylcholine Receptor, *Int. Rev. Neurobiol. 78*, 225−246.
9. Quick, M. W., and Lester, R. A. (2002) Desensitization of neuronal nicotinic receptors, *J. Neurobiol. 53*, 457−478.
10. Husain, S. S., Forman, S. A., Kloczewiak, M. A., Addona, G. H., Olsen, R. W., Pratt, M. B., Cohen, J. B., and Miller, K. W. (1999) Synthesis and properties of 3-(2-hydroxyethyl)-3-n-pentyldiazirine, a photoactivable general anesthetic, *J. Med. Chem. 42*, 3300−3307.
11. Pratt, M. B., Husain, S. S., Miller, K. W., and Cohen, J. B. (2000) Identification of sites of incorporation in the nicotinic acetylcholine receptor of a photoactivatible general anesthetic, *J. Biol. Chem. 275*, 29441−29451.
12. Forman, S. A., Miller, K. W., and Yellen, G. (1995) A discrete site for general anesthetics on a postsynaptic receptor, *Mol. Pharmacol. 48*, 574−581.
13. Dilger, J. P., Vidal, A. M., Mody, H. I., and Liu, Y. (1994) Evidence for direct actions of general anesthetics on an ion channel protein. A new look at a unified mechanism of action, *Anesthesiology 81*, 431−442.
14. Zhou, Q. L., Zhou, Q., and Forman, S. A. (2000) The n-alcohol site in the nicotinic receptor pore is a hydrophobic patch. *Biochemistry 39*, 14920−14926.
15. Forman, S. A. (1997) Homologous mutations on different subunits cause unequal but additive effects on n-alcohol block in the nicotinic receptor pore, *Biophys. J. 72*, 2170−2179.
16. Firestone, L. L., Alifimoff, J. K., and Miller, K. W. (1994) Does general anesthetic-induced desensitization of the Torpedo acetylcholine receptor correlate with lipid disordering?, *Mol. Pharmacol. 46*, 508−515.
17. Imoto, K., Busch, C., Sakmann, B., Mishina, M., Konno, T., Nakai, J., Bujo, H., Mori, Y., Fukuda, K., and Numa, S. (1988) Rings of negatively charged amino acids determine the acetylcholine receptor channel conductance, *Nature 335*, 645−648.
18. Grosman, C., Salamone, F. N., Sine, S. M., and Auerbach, A. (2000) The extracellular linker of muscle acetylcholine receptor channels is a gating control element, *J. Gen. Physiol. 116*, 327−340.
19. Kash, T. L., Jenkins, A., Kelley, J. C., Trudell, J. R., and Harrison, N. L. (2003) Coupling of agonist binding to channel gating in the GABA(A) receptor, *Nature 421*, 272−275.
20. Forman, S. A. (1999) A hydrophobic photolabel inhibits nicotinic acetylcholine receptors via open-channel block following a slow step, *Biochemistry 38*, 14559−14564.
21. Scheller, M., and Forman, S. A. (2002) Coupled and uncoupled gating and desensitization effects by pore domain mutations in GABA(A) receptors, *J. Neurosci. 22*, 8411−8421.
22. Brown, R. L., Gerber, W. V., and Karpen, J. W. (1993) Specific labeling and permanent activation of the retinal rod cGMP-activated channel by the photoaffinity analog 8-p-azidophenacylthio-cGMP, *Proc. Natl. Acad. Sci. U.S.A. 90*, 5369−5373.
23. He, Y., and Karpen, J. W. (2001) Probing the interactions between cAMP and cGMP in cyclic nucleotide-gated channels using covalently tethered ligands, *Biochemistry 40*, 286−295.
24. Mourot, A., Rodrigo, J., Kotzyba-Hibert, F., Bertrand, S., Bertrand, D., and Goeldner, M. (2006) Probing the reorganization of the nicotinic acetylcholine receptor during desensitization by time-resolved covalent labeling using [3H]AC5, a photoactivatable agonist, *Mol. Pharmacol. 69*, 452−461.
25. Mourot, A., Kotzyba-Hibert, F., Goeldner, M., and Bamberg, E. (2006) Photo-induced covalent attachment of agonists as a tool to study allosteric mechanisms of nicotinic acetylcholine receptors, *J. Mol. Neurosci. 30*, 3−4.
26. Ziebell, M. R., Nirthanan, S., Husain, S. S., Miller, K. W., and Cohen, J. B. (2004) Identification of binding sites in the nicotinic acetylcholine receptor for [3H]azietomidate, a photoactivatable general anesthetic, *J. Biol. Chem. 279*, 17640−17649.
27. Spitzmaul, G., Dilger, J. P., and Bouzat, C. (2001) The noncompetitive inhibitor quinacrine modifies the desensitization kinetics of muscle acetylcholine receptors, *Mol. Pharmacol. 60*, 235−243.
28. Arias, H. R., Bhumireddy, P., Spitzmaul, G., Trudell, J. R., and Bouzat, C. (2006) Molecular mechanisms and binding site location for the noncompetitive antagonist crystal violet on nicotinic acetylcholine receptors, *Biochemistry 45*, 2014−2026.
29. Auerbach, A., and Akk, G. (1998) Desensitization of mouse nicotinic acetylcholine receptor channels. A two-gate mechanism, *J. Gen. Physiol. 112*, 181−197.
30. Grosman, C., Zhou, M., and Auerbach, A. (2000) Mapping the conformational wave of acetylcholine receptor channel gating, *Nature 403*, 773−776.
31. Bianchi, M. T., and Macdonald, R. L. (2001) Mutation of the 9′ leucine in the GABA(A) receptor gamma2L subunit produces an apparent decrease in desensitization by stabilizing open states without altering desensitized states, *Neuropharmacology 41*, 737−744.
32. Chang, Y., and Weiss, D. S. (1999) Allosteric activation mechanism of the alpha1beta2gamma2 gamma-aminobutyric acid type A receptor revealed by mutation of the conserved M2 leucine, *Biophys. J. 77*, 2542−2551.
33. Purohit, Y., and Grosman, C. (2006) Block of muscle nicotinic receptors by choline suggests that the activation and desensitization gates act as distinct molecular entities, *J. Gen. Physiol. 127*, 703−717.

BI701287A